**1. Shaik Ruksana Begam[1,2], 2. Loveswara Rao Burthi[1], 3. Shobha Rani Depuru[2]**

Koneru Lakshmaiah Education Foundation (1), Institute of Aeronautical Engineering (2)
ORCID: 1. 0000-0001-5161-4086; 2. 0000-0002-1094-2208; 3. 0000-0001-8235-9671

doi:10.15199/48.2024.08.42

# Simulation and Hardware implementation of Novel Controller in dectric vehicle applications to improve system efficiency

***Abstract***. *Control techniques were essential to use converters to get the desired power and performance in electric vehicles' propulsion systems. To obtain a quicker transient response than that of other existing controllers, a novel controller DC-DC boost converter with Adaptive Neuro-Fuzzy rules that feds BLDCM (Brush Less Direct Current Motor) simulated and hardware designed to be robust and to have a steady-state response in electric propulsion of electric vehicles has been simulated and hardware implementation also done in this work. The MOSFET (Metal-Oxide-Semiconductor Fed-Effect Transistor) used in the proposed controller acts like a switch to determine operational mode. The proposed controllers' performance analysis was carried out with that of output voltage, components and number of switches used, electromagnetic torque, reliability,and system cost. The converter output voltage is controlled by the proposed ANF-SM controller as per the required speed in EV. As per the results with simulation and hardware implementation waveform results, the results of simulation and hardware implementation inferred that the proposed controller functions well with input and under different loaded conditions when compared to other traditional controllers. In a comparative analysis,the proposed non-linear boost converter was better than that of other existing controllers. It can be concluded that non-linear control with DC-DC boost-converters fed with the BLDC motor was more suitable for electric propulsion of electric vehicles.*

**Streszczenie.** *Techniki sterowania były niezbędne do wykorzystania przetwornic w celu uzyskania pożądanej mocy i wydajności w układach napędowych pojazdów elektrycznych. Aby uzyskać szybszą reakcję na stany przejściowe niż w przypadku innych istniejących sterowników, zastosowano nowatorski konwerter podwyższający DC-DC sterownika z adaptacyjnymi regułami Neuro-Fuzzy który zasila symulację BLDCM (brush less direct current motor) oraz sprzęt zaprojektowany tak, aby był solidny i zapewniał stałą reakcję w napędzie elektrycznym pojazdów elektrycznych, a w ramach tej pracy przeprowadzono również implementację sprzętu. MOSFET (tranzystor z efektem metalowo-tlenkowo-półprzewodnikowym) zastosowany w proponowanym sterowniku działa jak przełącznik określający tryb pracy. Analizę wydajności proponowanych sterowników przeprowadzono z uwzględnieniem napięcia wyjściowego, komponentów i liczby zastosowanych przełączników, momentu elektromagnetycznego, niezawodności i kosztu systemu. Napięcie wyjściowe przetwornicy jest kontrolowane przez proponowany sterownik ANF-SM w zależności od wymaganej prędkości w EV. Zgodnie z wynikami symulacji i wynikami przebiegów implementacji sprzętu, z wyników symulacji i implementacji sprzętu wynika, że proponowany sterownik działa dobrze z wejściem i przy różnych warunkach obciążenia w porównaniu z innymi tradycyjnymi sterownikami. W analizie porównawczej zaproponowany nieliniowy konwerter podwyższający okazał się lepszy od innych istniejących sterowników. Można stwierdzić, że w przypadku elektrycznego napędu pojazdów elektrycznych bardziej odpowiednie było sterowanie nieliniowe za pomocą przetwornic podwyższających napięcie DC-DC zasilanych silnikiem BLDC.* (***Symulacja i implementacja sprzętowa nowatorskiego sterownika w zastosowaniach pojazdów elektrycznych w celu poprawy wydajności systemu***)

**Keywords:** Full bridge DC-DC boost-converter, PMBLDCM motor, ANF-SMC controller, MOSFET switch, non-linear boost-converter.
**Słowa kluczowe**: Pełnomostkowy konwerter podwyższający DC-DC, silnik PMBLDCM, kontroler ANF-SMC, przełącznik MOSFET,:

## 1. Introduction

In the transportation zone natural resources lead to the design, implementation, and comparative analysis of alternative electrical propulsion of electric and hybrid electric vehicles [1 to 4], global research carried out on energy efficiency in EVs for complete replacement of conventional IC engines. In the development of EVs much concentrated on the design of converters, batteries, and power electronics for minimizing cost Implementation of the best power control strategy is essential to solve major problems and to increase the performance and better driving style of electric vehicles, the motor should be efficient and lightweight weight [5] with an advanced cooling system. Power flow regulated in electric propulsion using a hybrid energy storage system proposed in [6], for increasing efficiency of power train with ultra-efficient energy system proposed in [7], usage of polyphase motors for improving reliability proposed in [8], dual motor coupling system to improve the efficiency proposed in [9], to improve range of vehicle BLDCM with dual stator and rotor winding proposed in [10]. This proposed system simulation with hardware implementation in an electric propulsion subsystem for cost-effectiveness and improved vehicle efficiency, is used where electrical isolation is required and for high power transmission. DC-DC boost converter converts DC power (200V-800V) from high voltage battery to lower voltages (48V to 12V) for head and interior lights, wipers, window motors, fans, pumps, and other elementsin the EV, whereas buck-boost and Cuk converters were used for both purposes. In electric vehicles, less current is required when the voltage is higher. [11 – 14] proposed how to achieve a higher efficiency motor driving system with the usage of the additional boost converter. With the usage of conventional boost converters energy won't transfer to charge the battery. In medium and high-power vehicles non-isolated DC- DC converters were used due to their simpler architecture and accessible control strategy. If the DC Voltage gain is < 4% (boost, buck-boost, Cuk, and SEPIC converters) these four converts were available, them boost DC-DC converter (BC) mostly employed power converter SMPS as step-up the input voltage, in the case of step-down the current posses at least one energy storage element with a diode and a switch as shown in “Fig. 1”. BC has many advantages such as moderate output voltage (< 4%) can be obtained, the switch can be driven easily, filtering can be done easily, continuous input current and at fool load moderate efficiency can be obtained. The limitations of this converter are not suitable for high voltage gains (>4%) and weight moderately heavy.

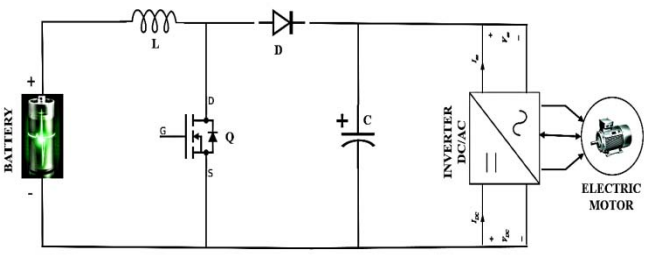


Fig 1 Design description of used (BC) converter

Two working modes of BC, which are switched ON and OFF modes, in the case of switched-on mode the gate will be active

The current will flow with the inductor, energy stored with the generation of the magnetic field, as in the second mode gate is inactive and current flows through the load. Equations used in two modes were described as follows:
The equation used in mode1 (switched on mode):

(1) $V_{(input)} - L(\Delta/ton) = 0$

The equation used in mode2 (switched off mode):

(2) $V_{(input)} - V_{(out)} = L\ (\Delta/tof\ f)$ ----------

(3) $V_C = \frac{1}{C}\int_0^{ton} ic\,dt + Vc\ (t = 0)$

Considering average capacitor current during on time as $I_0$,
derived the final equation for L and C as:

(4) $L = \frac{(1-D)\ X\ Vout}{fsw\ X\ \Delta Illmax}$ ----------

(5) $C = \frac{D\ X\ Iout}{fsw\ X\ \Delta Vout}$ ----------

And duty cycle calculated as

(6) $D = 1 - (V_{in} / V_{out})$ ----------

In this proposed work converter with a non-linear controller is used for driving a PMBLDC motor. For smooth dandling in case of heavy loads and with higher torques, the size of the EV motor will depend on rolling speed, aerodynamic drag, hill climbing, and acceleration rolling resistance, the proposed linear mechanism in [15], proposed non-linear controllers in [16] and performances of both types of converters implemented in [17]. Implementation of real-time DC-DC converter for prototype development with low-power rating referred to in [18]. The work consists of six sections, which introduction and literature survey, a design description of the converter is covered in section 1, a design and simulation description of the proposed system and its sub-system, and a BLDC motor description, in section 2. Section 3 is an architectural description of the two types of controllers, and results obtained with simulation implementation and discussion. In section 4 Hardware setup, implementation, and its results are discussed. Section 5 Conclusion, and future work were presented.

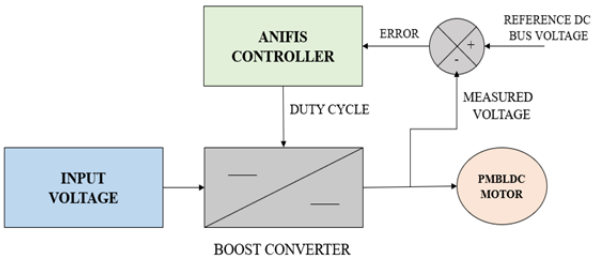


Fig. 2 Design Description of used Converter with proposed control strategy in the system

## 2. Design Description and Simulating the proposed system and its sub-system

### 2.1 Design Description of used Converter with Control Strategies

Fig. 2" describes the used system consisting of three main components DC input, used converter, and the PMBLDC motor with a non-linear control strategy as shown. The proposed system will control output voltage results with the used converter as in the case of input voltage variations or changes in the load based on time. The used converter takes the voltage of input from the direct current and duty cycle from the proposed non-linear control strategy and gives the output to the used PMBLDC motor. In the case of motor operation, it is very important to maintain a constant input voltage in driving the PMBLDC motor. "Table 1", used the design parameters that were described.

Table 1 Describing used Design Parameters

| | |
|---|---|
| Used Non-linear Converter I/P voltage | 9.000 V |
| Full bridge DC-DC boost converter voltage | 12.000 V |
| O/P Power in watts | 12.000 W |
| Rating of PMBLDC motor | 12.000 V, 3K RPM |
| Frequency in Kelo hearts | 25.000 KHz |
| % of duty cycle | 25.000 |

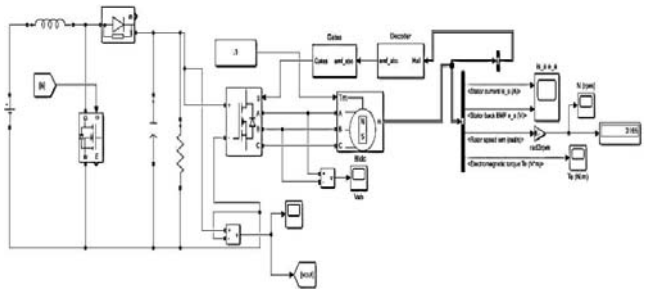

Fig. 3.1 Description of Proposed System Simulation Model

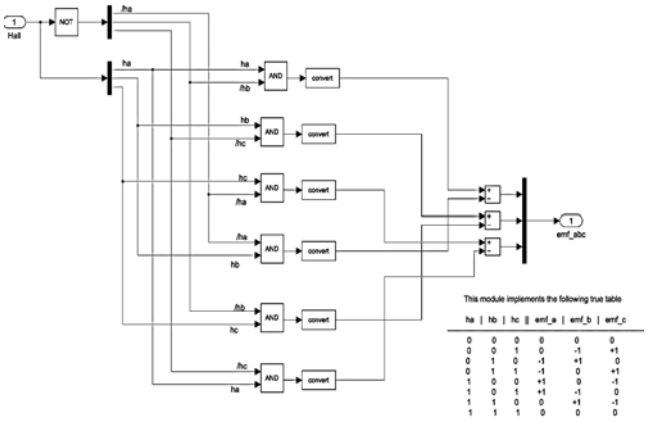

Fig. 3.2 Description of Proposed System's sub-system Diagram Hall effect and its truth table

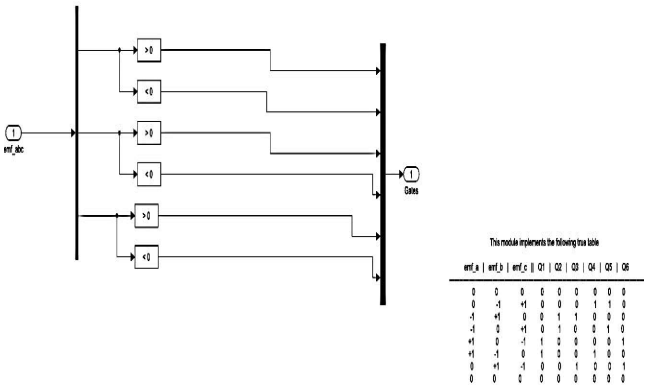

Fig. 3.3 Description of Proposed System's Diagram and sub-system decoder and its truth table

### 2. 2 Design Description of Simulation Model of the proposed system and its subsystems

The design description and its subsystem are in "Fig. 3". The proposed system is described in "Fig. 3.1" which has an inverter that converts AC to DC, which will be input to the system from which it will go to the BLDC motor, it will also consist of Gates and Decoder. From this, the output will be displayed in four scopes, in which scope1 displays

the stator current and stator back EMF, scope2 and scope4 display the rotor speed, and scope3 displays the electromagnetic torque.

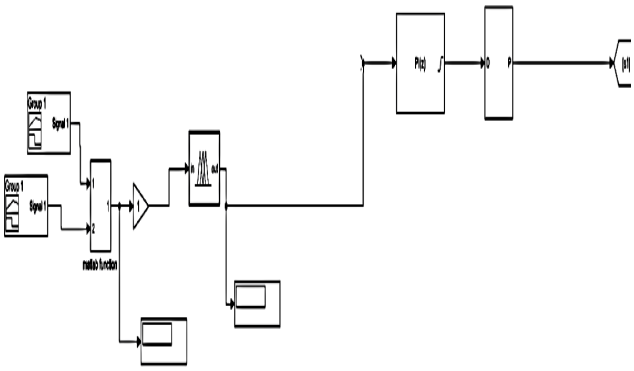

Fig. 3.4 Description of Proposed Simulation Model of Fuzzy Fuzzy System

Fig. 3 Design Description of Simulation Model of the proposed system and its subsystems

"Fig. 3.2" describes the proposed subsystem's Hall effect and its truth table with the values of ha, hb, and hc and their emf-a, emf-b, and emf-c values. In "Fig. 3.3" the subsystem's decoder and its truth table with values of emf-a to emf-c values from "Fig. 3.2" and values of Q1 to Q6 were shown. "Fig. 3.4" describes the proposed system simulation diagram with the Fuzzy subsystem which has two input signals, the MATLAB function subsystem and the controllers used in the proposed system. "Fig. 3.5", describes the fuzzy sub-system of the proposed model which has two signal inputs one signal output will be input to the voltage filter, its output will be Vn, and another signal output acts as input of the current filter In. The final output values Vn-Vb, and In-Ib act as input to the Fuzzy sub-system. In "Fig. 3.6", the description of the proposed fuzzy sub-system ANFIS model structure with two inputs (Tmin and Tmax) each input will have three membership functions, and each membership function with three fuzzy rules and overall, with only 9 fuzzy rules were used in the proposed system.

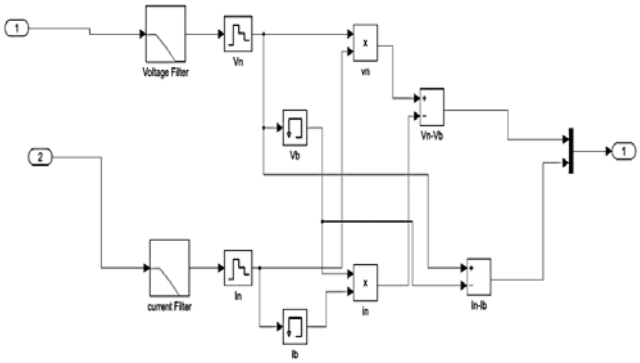


Fig. 3.5 Description of Simulation Model of the Proposed Fuzzy sub-system Diagram

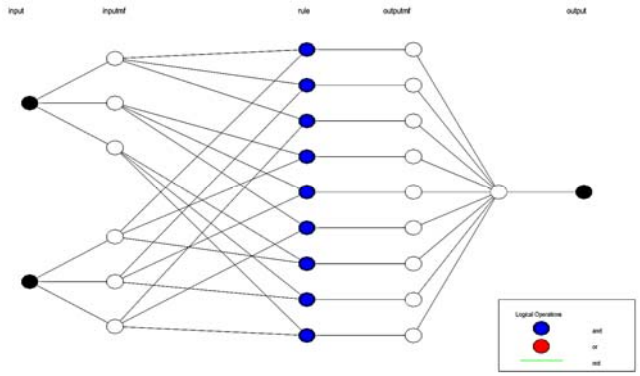


Fig. 3.6 Description of Simulation Model Diagram of the Proposed Fuzzy sub-system ANFIS Model Structure Diagram

Table 2 Description of the used Workspace Details

| Dec | Value | Description | Value | Description | Value |
|---|---|---|---|---|---|
| Alpha | 0.08699800 | Beta | -0.369010000000000 | Data | 1000x3 double |
| G | 9.91306921184190e+02 | Gmax | 1000 | Gmin | 0 |
| Gs | 1000 | i | 1000 | IMP | 1x1000 double |
| IMPS | 8.150000000000000 | Input | 1000x2 double | ISCS | 8.660000000000000 |
| OP | 1000x1 double | OP1 | 1000x1 double | Output2 | 1000x1 double |
| PMP | 1x1000 double | T | 18.001934453252670 | Tmax | 35 |
| Tmin | 15 | Ts | 25 | VMP | 1x1000 double |
| VMPS | 30.70000000000000 | VOCS | 37.300000000000000 | ---------- | ---------- |

**2.3 Steps in Neuro-Fuzzy Designer**
Step1: Load Dataset
Step2: Generate FIS
Step3: Train FIS keeping Error Tolerance as 0 and Epochs as 10 to 100
Step4: Test FIS
Step5: Export and Execute File
Step6: Find Rotor Speed, Electromagnetic Force, Electromagnetic Torque and Stator Current Results
Table 2" describes the workspace details and their values used in the proposed ANF-SMC controller.

**2.4 Steps Involved in Adaptive Neuro-Fuzzy Algorithm**
**Step 1:** Initialize the values of ISCS, IMPS, VOCS, VMPS, alpha, beta, Gs, and Ts.

**Step2:** Repeat the process for values of i=1 to 1000 with the following steps
**2.1** Initialize Tmin, and Tmax values and calculate Temperature T = (Tmax-Tmin)*rand + Tmin
**2.2** Initialize Gmin, and Gmax values and calculate Irradiance G = (Gmax-Gmin)*rand+ Gmin
**2.3** Calculate maximum current, voltage, and power as Follows

```
IMP(i) =IMPS* (G/Gs)*(1+(alpha* (T-Ts)))
VMP(i)=VMPS+(beta*(T-Ts))
PMP(i)=VMP(i)*IMP(i)
```

**2.4** Compute input based on irradiance (G) and temperature (T) values.
**2.5** Compute output (VMP), (IMP), (PMP) and data (G T VMP)

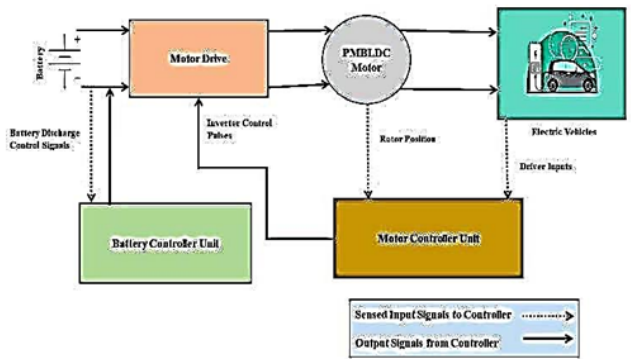


Fig. 4 Used PMBLDC motor Description

### 2.5 PMBLDC motor block diagram and mathematical descriptio

In “Fig. 4” a description of the PMBLDC motor was done, in which set input and control signals were represented with dotted lines whereas output signals were represented with thick lines from the controller. In this block diagram, various units such as EVs, motors and drives, batteries, and controllers were represented. The motor is driven to the battery controller unit when an input signal is sent from the electric vehicle to the PMBLDC motor. The processed output signals will be sent from the battery and controller to the motor drive, from there to the PMBLDC motor and electric vehicle. The mathematical model of the PMBLDC motor is described as

The phase voltage of PMBLDCMs is represented as
Applied Phase Voltage (V) = Resistance of stator (R)* Current of phase (I) + inductance (S) + torque (T) + Current of phase (I) + Voltage of Back EMF (E) ---------- (1)

Applied Phase Voltage (V) = $[V_a V_b V_c]^T$

Resistance of stator (R) = diag[R]

Current of phase (I) = $[I_a I_b I_c]^T$ and

The voltage of Back EMF (E) = $[E_a E_b E_c]^T$ of PMBLDCM motor

The Matrix Inductance will be represented as shown below.

$$S=\begin{bmatrix} SI(L)-MI(M) & 0 & 0 \\ 0 & SI(L)-MI(M) & 0 \\ 0 & 0 & SI(L)-MI(M) \end{bmatrix} \ldots\ldots\ldots (2)$$

Where SI (L) and MI (M) are self and mutual inductance of PMBLDCM motor.

The Electro Magnetic Torque (EMT) of PMBLDCMs is represented as

$$emt = \frac{e_a I_a + e_a I_b + e_c I_c}{\omega_m} \ldots\ldots\ldots\ldots\ldots\ldots\ldots\ldots\ldots\ldots\ldots\ldots\ldots\ldots\ldots\ldots (3)$$

$$emf - load = \frac{d\omega_m}{dt} + V_{fr} \ldots\ldots\ldots\ldots\ldots\ldots\ldots\ldots\ldots\ldots\ldots\ldots\ldots\ldots\ldots\ldots\ldots\ldots (4)$$

Subscriptions can speed of the rotor ($\omega_m$) is calculated from equation (4)

$$\omega_m = \int \frac{T_{emf} - T_{load} - V_{fr\omega_m}}{J} dt \ldots\ldots\ldots\ldots\ldots\ldots\ldots\ldots\ldots\ldots\ldots\ldots\ldots\ldots\ldots\ldots (5)$$

Currently, the stator windings are shown as

$$\begin{bmatrix} I_a \\ I_b \\ I_c \end{bmatrix} = \begin{bmatrix} \sin(\omega_r t + \alpha) \\ \sin\left(\omega_r t + \alpha - \frac{2\pi}{3}\right) \\ \sin\left(\omega_r t + \alpha + \frac{2\pi}{3}\right) \end{bmatrix} I_{max} \ldots\ldots\ldots\ldots\ldots\ldots\ldots\ldots\ldots\ldots\ldots\ldots\ldots\ldots\ldots\ldots\ldots\ldots (6)$$

“Table 3" describes the used PMBLDC motor parameters and their specified values.

### 3.0 Architectural Description of used linear and non-linear Controllers

As the battery-operated devices in electric vehicles were increasing, demand for the usage of non-linear full bridge DC-DC boost converters increased. The proposed converter operated with a linear (PID), the ANF-SMC controller, and results were compared to perform comparative analysis

Table 3 The PMBLDC motor parameters used description

| Description of the PMBLDC Motor used design parameters | The Parameters values |
|---|---|
| Rating of power parameters | 8.000 W |
| Rating of voltage | 12.000 V |
| Resistance of Armature | 1.550 Ω |
| Inductance of Armature | 0.005 H |
| Inertia | $2.215 \times 10^{-5}$ kg m$^2$ |
| Value of Viscus Friction constant | $2.913 \times 10^{-6}$ N.m.s. |
| Torque and Voltage Constant Values | 1.800 Nm/A, 1.800 V/rpm |
| Value of Friction Torque | 0.100 |

### 3.1. PID Linear Controller Architectural Description

In “Fig. 5”, the simulation diagram of the linear PID controller is represented with constant parameters by employing the advantage of systems with non-linear differential equations as represented.

Equations related to PID control

$$f_1 = \int_0^{\infty} (e(t))^2 \, dt$$

$$f_2 = \frac{1}{\left[c_1(t_r - t_{rd}) + c_{2(M_p - M_{pd})} + c_3(t_s - t_{sd}) + c_4(e_{ss} - e_{ssd})\right]}$$

$$f_3 = \frac{1}{\left[(1 - e^{-\beta})(M_p - e_{ss}) + e^{-\beta}(t_s - t_r)\right]}$$

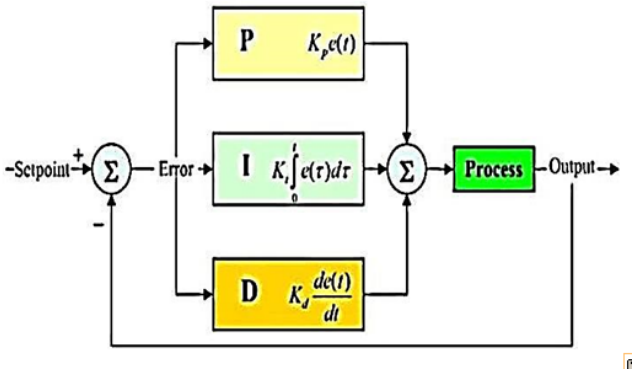


Fig. 5 PID Control Simulation Diagram

### 3.2. The ANF-SMC non-linear Controller Architectural Description

By using the proposed controller with a PMBLDC motor limitations in existing non-linear controllers can be overcome. Designing and implementation of the system and its sub-system using the MATLAB/Simulink R2020b tool along with the Takagi Sugano kit were represented in "Fig 3" and fuzzy rules of e/e' were described in "Table 4" and the truth table in "Table 5".

Table 4. Description of used Fuzzy rules with The Proposed ANF-SMC Controller of e/e'

| e/e' | inp2 mf1 | inp2 mf2 | inp2 mf3 | inp2 mf4 | inp2 mf5 |
|---|---|---|---|---|---|
| inp1 mf1 | oup1 mf1 | oup1 mf2 | oup1 mf3 | oup1 mf4 | oup1 mf5 |
| inp1 mf2 | oup1 mf6 | oup1 mf7 | oup1 mf8 | oup1 mf9 | oup1 mf10 |
| inp1 mf3 | oup1 mf11 | oup1 mf12 | oup1 mf13 | oup1 mf14 | oup1 mf15 |
| inp1 mf4 | oup1 mf16 | oup1 mf17 | oup1 mf18 | oup1 mf19 | oup1 mf20 |
| inp1 mf5 | oup1 mf21 | oup1 mf22 | oup1 mf23 | oup1 mf24 | oup1 mf25 |

Table 5. Description of Truth Table used in the proposed model

| | | | | | |
|---|---|---|---|---|---|
| 0.00 | 0.00 | 0.00 | 0.00 | 0.00 | 0.00 |
| 0.00 | 0.00 | 1.00 | 0.00 | -1.00 | +1.00 |
| 0.00 | 1.00 | 0.00 | -1.00 | +1.00 | 0.00 |
| 0.00 | 1.00 | 1.00 | -1.00 | 0.00 | +1.00 |
| 1.00 | 0.00 | 0.00 | +1.00 | 0.00 | -1.00 |
| 1.00 | 0.00 | 1.00 | +1.00 | -1.00 | 0.00 |
| 1.00 | 1.00 | 0.00 | 0.00 | +1.00 | -1.00 |
| 1.00 | 1.00 | 1.00 | 0.00 | 0.00 | 0.00 |

(a) Results with linear PID Controller

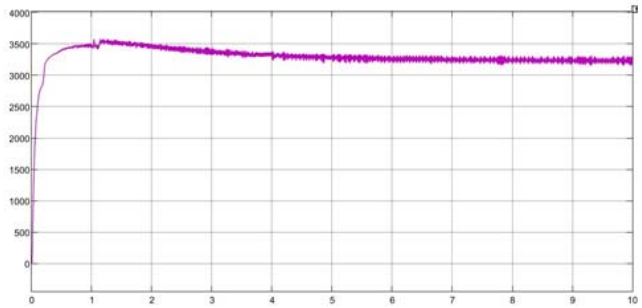

(b) Results with on-linear ANF-SMC Controller

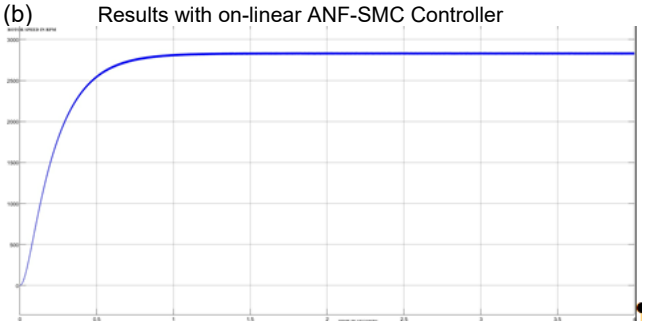

Fig. 6 Simulation results of Speed with linear PID and non-linear (ANF-SMC) using DC-DC converter with PMBLDC motor

### 3.3 Description of results obtained by the proposed controller

#### 3.3.1 Obtained Results and Discussion of Speed using non-linear (ANF-SMC) Controller with DC-DC converter

Simulation results with the PID controller are shown in "Fig 6(a)" by taking execution time (secs) on the X-axis and the Y-axis the speed in RPM. Speed within 1 second varied from 0 to 3500 RPM, up to 2 secs speed of 3.5 K RPM maintained, later it reduces from 3500 to 3200 RPM up to ten seconds. Simulation results with a non-linear (ANF-SMC) controller were shown in "Fig. 6(b)" by taking execution time (secs) on the X-axis and the Y-axis the speed in RPM. Speed within 1 second varied from 0 to 2800 RPM, later it remained constant up to ten secs. On observation of the obtained results, it can be inferred that in attaining constant speed the proposed controller takes very little time when compared to other existing controllers.

( a) Results with linear PID Controller

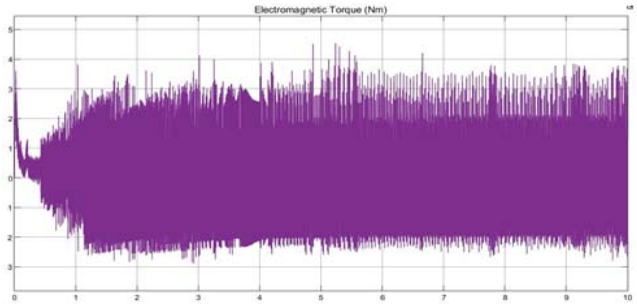


( a) Results with linear PID Controller

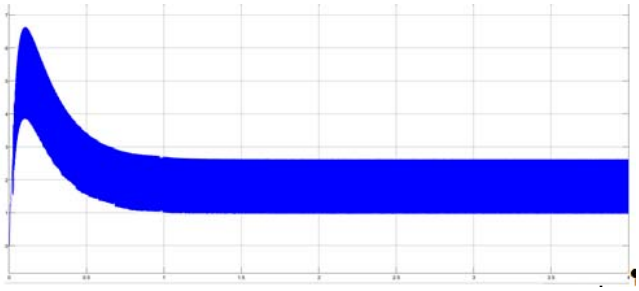

Fig. 7 Electro Magnetic Torque (EMT) with linear PID and non-linear (ANF-SMC) using DC-DC converter with PMBLDC motor.

#### 3.3.3 Simulation results and discussion of Stator Current using non-linear (ANF-SMC) controller with DC-DC converter

Simulation results of stator current with PID controller were shown in "Fig. 8(a)" by considering the time in seconds on the X-axis ranging from 0 to 0.2 secs with an interval of 0.002 sec, and electromagnetic torque on the Y-axis ranges

from -3.0 to +3.0 in ia with a speed of 3.5K rpm. On observation of results, the proposed controller within 0.01 secs stator current value changes from -2.2 ia to +2.0 ia, from 0.01sec to 0.05sec -1.0 to +1.0 ia, from 0.05 secs to 10 secs stator current values ranges from -1.0 to +1.0 to -2.0 to +2.5 continuously.

Simulation results of stator current with non-linear (ANF-SMC) controller were shown in "Fig. 8(b)" by considering the time in seconds on the X-axis ranging from 0 to 0.2 secs with an interval of 0.002 sec, and electromagnetic torque on the Y-axis ranges from -6.0 to +6.0 in ia with a speed of 3.5Krpm. On observation of results, the proposed controller maintains a constant stator current from 0 to 2 sec ranging from -2.1 to +2.1 continuously. On observation of results, the proposed controller maintains a constant stator current than that of another controller.

(a) Results with linear PID Controller

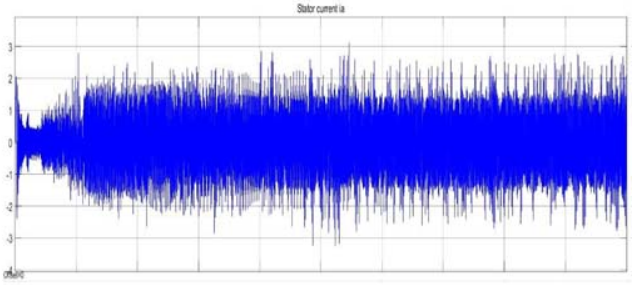


(b) Results with the proposed Non-linear (ANF-SMC) Controller

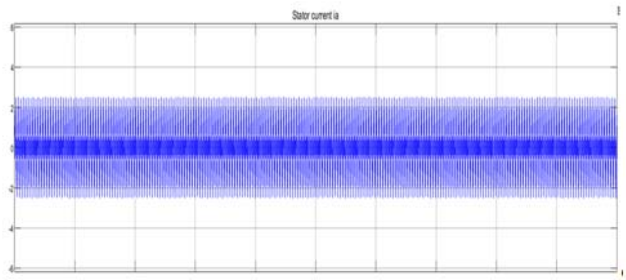


Fig. 8 Stator Current (SC) with linear PID and non-linear (ANF-SMC) using DC-DC converter with PMBLDC motor

### 3.3.4 Simulation results and discussion of Electromotive Force (EMF) in volts with non-linear (ANF-SMC) full bridge DC-DC converter

Simulation results of electromotive force (EMF) with PID controller were shown in "Fig. 9(a)" by considering the time in seconds on the X-axis ranging from 0 to 10 secs, and electromotive force on the Y-axis ranges from -150.0 to +150.0 volts with a speed of 3.5K rpm. On observation of results, the proposed controller from 0.0sec to 1.0 sec electromotive force will be constant at 150 volts from 1.0 secs to 10 secs electromotive force will be constant at 152 volts.

Simulation results of electromotive force (EMF) with a non-linear (ANF-SMC) controller were shown in "Fig. 9(b)" by considering the time in seconds on the X-axis ranging from 0 to 0.2 secs with an interval of 0.002 sec, and electromotive force on the Y-axis ranges from -1500.0 to +1500.0 volts with a speed of 3.5K rpm. On observation of results, the proposed controller from 0.0 sec to 0.2-sec electromotive force will be a constant value from -1400 to +1400 volts. On observation of results, the proposed controller maintains a constant electromagnetic force than that of another controller.

(a) Results with linear PID Controller

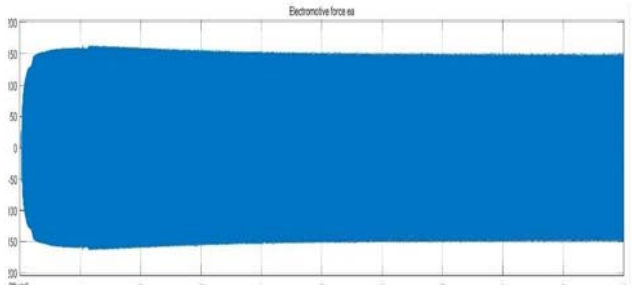


(b) Results with linear PID Controller

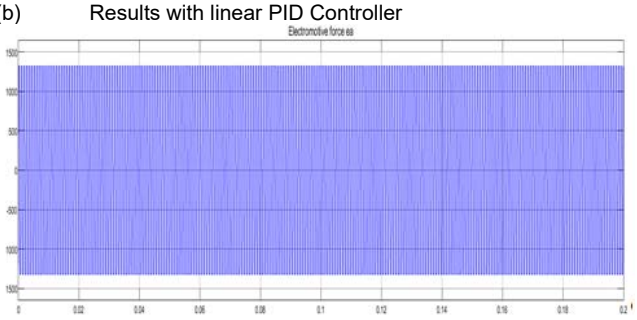


Fig. 9 Simulation results of Electromotive Force (EMF) in volts, with linear PID and non-linear (ANF-SMC) full bridge DC-DC converter

(a) Trained Data FIS Input Diagram

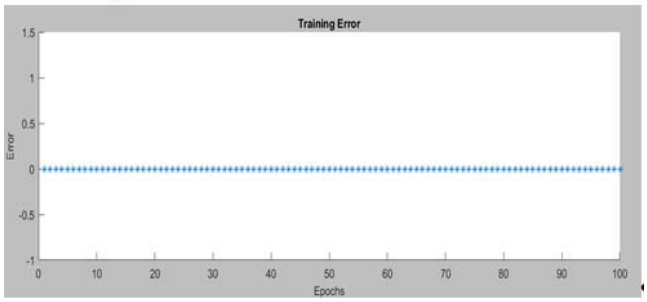


(b) Trained Data FIS Input Diagram

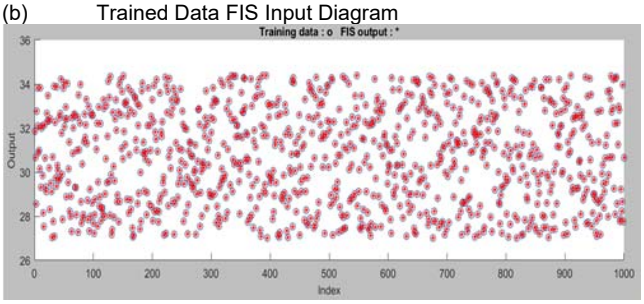


(c) Trained Data FIS Input Diagram

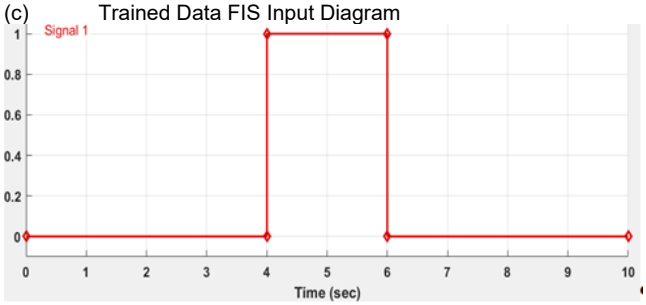


Fig. 10 Simulation results of Trained Data FIS input and output diagrams, signal builder diagram of non-linear (ANF-SMC) controller with DC-DC converter.

### 3.3.5 Simulation results and discussion of Trained Data FIS input and output diagrams, signal builder diagram of non-linear (ANF-SMC) controller with DC-DC converter

In “Fig 10(a)” Trained Data FIS input diagram is represented by taking several epochs on the X-axis ranging from 0 to 100 and taking Error values ranging from -1 to +1.5. On observation of results, the proposed controller maintains 0 error irrespective of the number of epochs.

In “Fig 10(b)” Train Data FIS output diagram is represented by taking index values ranging from 0 to 1000 with an interval of 100 and taking output values on the Y-axis ranging from 27 to 34. On observation of results, the proposed controller maintains the same range of output irrespective of the index value.

In “Fig 10(c)” signal builder diagram is represented by taking time in a sec on the X-axis ranging from 0 to 10 sec, and signal1 vale on the Y-axis ranging from 0 to 1 with an interval of 0.2. On observation of results the proposed controller signal value will be 0 from 0 to 4 sec, from 4 to 6 it will be constant with 1, and from 6 to 10 sec it will be 0.

## 4. Hardware Implementation and Results Discussion

### 4.1 Description of Hardware setup and implementation

In “Fig 11(a)” input sine wave, “Fig 11(b)” inverter output and “Fig 11( c)” proposed system pulse circuit with a BLDC motor speed of 3500 RPM and DC-DC boost converter were represented.

(a) Input Sine Wave

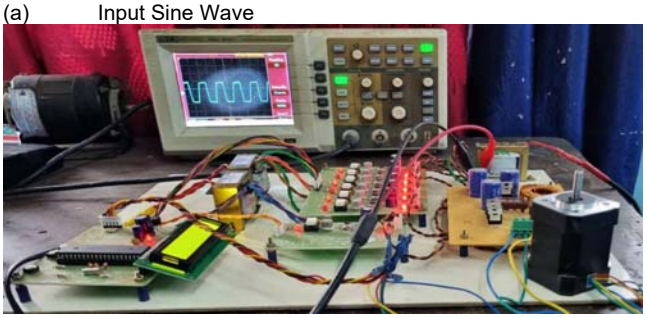

(b) Inverter Output

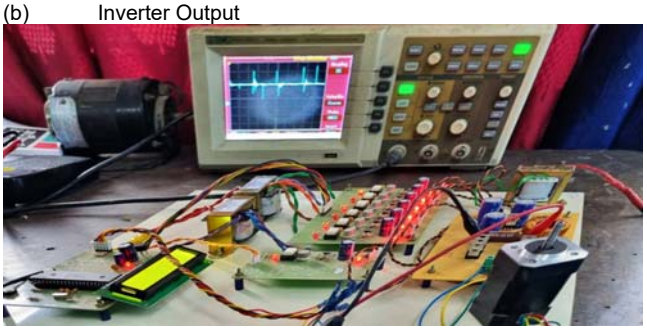

(c ) Pulse Circuit

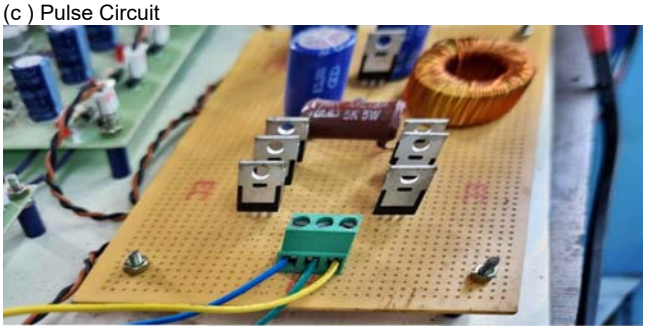

Fig. 11 Description of Hardware setup of proposed system Non-linear controller (ANF-SMC) with BLDC motor speed of 3500 RPM and DC-DC boost converter used.

(a) BLDC motor ( 1 . 5 K R P M ) CONTROL with DC-DC boost converter Duty = 12, Speed = 134 RPM

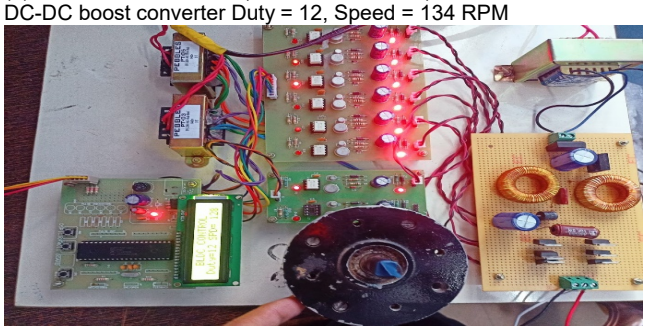

(b) BLDC motor ( 1 . 5 K R P M ) CONTROL with DC-DC boost converter Duty = 12, Speed = 134 RPM

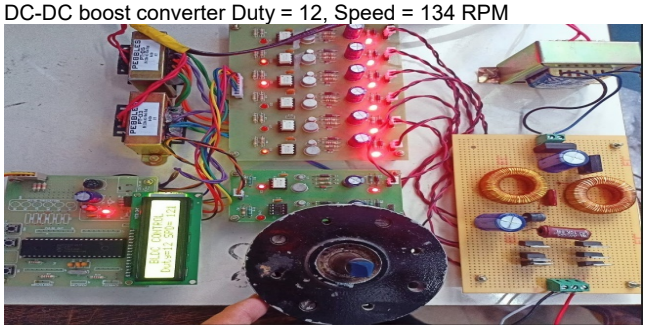

(c) BLDC motor ( 1 . 5 K R P M ) C O N T R O L with DC-DC boost converter Duty = 12, Speed = 138 RPM


(d) BLDC motor ( 1 . 5 K R P M ) C O N T R O L with DC-DC boost converter Duty = 12, Speed = 138 RPM


Fig. 12 Description of Hardware setup of proposed system Non-linear controller (ANF-SMC) with BLDC motor speed of 1500 RPM and used converter.

Hardware setup of a BLDC motor control with used converter of 12 volts duty is used with different speeds (134, 121, 138 and 803 rpm) shown in “Fig. 12(a) to 12(d)” respectively. The output results of the simulation in terms of scope, speed, stator current electromagnetic force, and torque are shown in “Fig.13”.

Speed Results were described in “Fig. 13(a)” by considering time on X-axis values ranging from 0 to 4 seconds with an interval of 0.5 sec, and speed values ranging from 0 to 4000 RPM with an interval of 500. With the results, it can be inferred that as the time increases from 0 sec to 2.5 sec, the speed value graduallyincreases from 0

to 3750, after 2.5 secs to 4.0 secs the value gradually decreases from 3750 to 3500, and from there on it will be a constant speed of 3500 RPM.

Stator Current and Electro Magnetic Force Results are described in “Fig. 13(b)”. As in the case of both Stator Current and Electro Magnetic Force by considering time on X-axis values ranging from 2.0 to 2.11 seconds with an interval of 0.002 sec, as in the case of Y-axis values the stator current values ranging from -0.5 to +0.5 with an interval of 0.1and in case of Electromagnetic Force values ranges from -200 to +200. With the results it can be inferred that as the time increases from 0 sec to 2.0025 sec, the stator current value gradually increases with fluctuations from -4.0 to +4.0, and after 2.0025 secs to 2.0045 secs the value gradually decreases from +4.0 to -4.0, from 2.0045 sec to 2.0007 sec, the stator current value gradually increased with fluctuations from -4.0 to +4.0, from 2.0007 sec to 2.100 sec, the stator current value gradually decreased with fluctuations from +4.0 to -4.0, from 2.100 sec to 2.1045 sec, the stator current value gradually increased with fluctuations from -4.0 to +4.0, from 2.1045 sec to 2.1065 sec, the stator current value gradually decreased with fluctuations from +4.0 to -4.0, from 2.1065 sec to 2.1105 sec, the stator current value gradually increased with fluctuations from -4.0 to +4.0. With the results of Electromagnetic Torque time from 1.95 sec to 2.0035 the results will be in trapezoidal form values ranging from (-160 to +160, +160 to -160 volts), on the whole time from 1.95 sec to 2.12 sec the Electromagnetic Force values will be from -160 to +160 in the form of Quora.

(a) Result of Speed

(b) Result of Stator Current and Electro-Magnetic Force

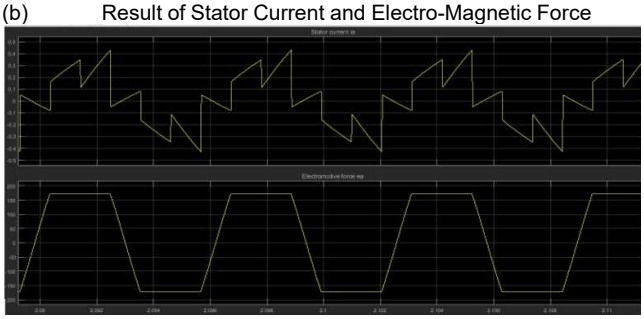

(c) Result of Electromagnetic Torque

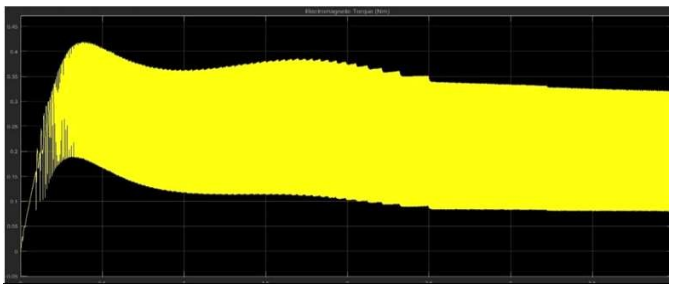

Fig. 13 Description of the Proposed Controller’s Hardware results of BLDC motor with DC-DC converter

Electromagnetic Torque Results were described in “Fig 13(c)” by considering time on the X-axis ranging from 0 sec to 4 sec with an interval of 0.5 sec and on the Y-axis Electromagnetic Values 0 to 0.45 Nm with a range of 0.05. On observation of results of the proposed controller as the time increases from 0 sec to 0.3 secs the EMT value will be 0, after 0.1 sec its value changes from 0.1 to 0.42 Nm, from 0.1 sec to 2.5 sec the value changes from 1.7 to 0.1, 0.42 to 0.34 Nm. From there on words the EMT value will be maintained constantly from 0.08 to 0.37 Nm.

In “Fig. 14” output results of the proposed controller with hardware setup were represented.

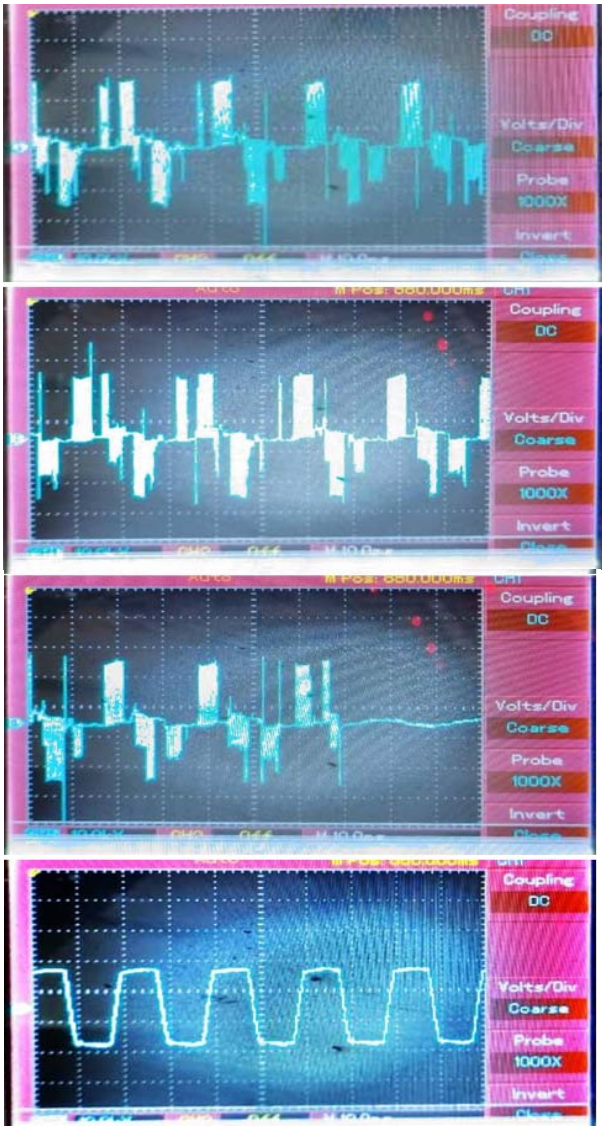


Fig. 14 Description of got output with Hardware setup used in a proposed system in the waveforms

## 5. Conclusion and Future Scope

To control the output voltage generated by the used converter during the drive cycle and to reduce the losses at the used motor side, within the work proposed novel controller ANF-SMC using DC-DC converter which feds used BLDC motor is simulated and hardware implementation was carried out. The proposed system and subsystem comparative analysis study done with that of existing linear and non-linear controllers in terms of output voltage, EMT, reliability, and cost was also performed. It can be perceived from the results in the case of simulation, hardware implementation, output waveforms, analysis, and

time domain specification that the proposed novel controller performs well as in the case of input and load variations when used with adaptive neuro principles. It can be concluded that the proposed controller with DC-DC boost converters is more suitable for EV applications. In this work, a BLDC motor control with a DC-DC boost converter having 12 volts duty is used, when the required speed is greater than 20.00 KMPH, the used DC-DC converter comes into action to boost the voltage as per the required speed so that the current flow can also be reduced, which also reduce losses and improve the system performance of the system drive train.

In future work, this can also be tested with other types of controllers. In future work performance comparison during regenerative braking mode of EVs can also be tested. Multiple storage devices such as the battery, and supercapacitor, with a laboratory scale property, can be used in the analysis of the converter.

***Acknowledgements***

*This work has not received any grants by any means. In the declaration regarding the publication of work, authors have no conflict of interest and express their thanks for the efforts of editors and reviewers in timely response and valuable comments.*

***Authors:*** *Ms Shaik Ruksana Begum, Assistant Professor, EEE Department, Institute of Aeronautical Engineering, Hyderabad and Research Scholar in Koneru Lakshmaiah Education Foundation, Guntur, Email: ruksanabegam@iare.ac.in, Dr Loveswara Rao Burthi, Professor, EEE department, Koneru Lakshmaiah Education Foundation, Deemed to be University, Guntur, Email: loveswararao@kluniversity.in, Dr Shobha Rani Depuru, Professor, EEE Department, Institute of Aeronautical Engineering*

REFERENCES

1 G Young-Joo Lee, Alireza Kaleigh, Ali Emadi, “Advanced Integrated Bidirectional AC/DC and DC/DC Converter for Plug-In Hybrid Electric Vehicles,” *IEEE Transactions on Vehicular Technology*, vol. 58, no.8, pp. 3970-3980, October 2009.

2 Emadi, Ali, Kaushik Rajasekhara, Sheldon S. Williamson, and Srdjan M. Lukic, \Topological overview of hybrid electric and fuel cell vehicular power system architectures and conjurations, "*IEEE Transactions on Vehicular Technology*, 54, no. 3 (2005): 763-770.

3 Chan, C. C., Alain Bouscayrol, and Keyu Chen, \Electric, hybrid, and fuel-cell vehicles: Architectures and modelling," *IEEE Transactions on Vehicular Technology*, 59, no. 2 (2010):589-598.

4 Emadi, Ali, Young Joo Lee, and Kaushik Rajasekhara, \Power electronics and motor drives in electric, hybrid electric, and plug-in hybrid electric vehicles, "*IEEE Transactions on Industrial Electronics*, 55, no.6 (2008): 2237-2245.

5 Martin Doppel Bauer and Patrick Winzer, "A lighter motor for tomorrow's electric car," EEE Spectrum, June 22, 2017.

6 Begam, S.R., Loveswara Rao, B. & Shobha Rani, D. ANF-RBC Controller to Regulate Power Flow of Electric Propulsion in Electric Vehicles. *Int. J Automot.Technol.***24**,1213–1221(2023). https://doi.org/10.1007/s12239-023-0099-1.

7 Yukihiro Tanaka, Yukinori Tsuruta, Takahiro Nozaki and Atsuo Kawamura, "Proposal of ultra-high efficient energy conversion system (HEECS) for electric vehicle power train," 2015 IEEE International Conferenceon Mechatronics (ICM)., 20 April 2015.

8 Nandor Bodo, Emil Levi, Ivan Subotic, Jordi Espina, Lee Empringham, and C. Mark Johnson, " Efficiency Evaluation of Fully Integrated On-Board EV Battery Chargers With Nine-Phase Machines," IEEE Transactions on Energy Conversion, vol. 32, no. 1, March 2017.

9 Minghui Hu, Jianfeng Zeng, Shaozhi Xu, Chunyun Fu and Datong Qin, “Efficiency Study of a Dual-Motor Coupling EV Powertrain," IEEE Transactions on Vehicular Technology Volume: 64, Issue: 6, June 2015.

10 B. V. Ravi Kumar, K Sivakumar, S.Karunanidhi, “ A Novel Configuration of Regenerative Braking System to improve the Energy efficiency of an Electric Vehicle with Dual-Stator Dual-Rotor BLDC motor”,2017 IEEE Transportation Electrification Conference.

11 Siddharth Mehta, Harsh Mittal, Nithya Venkatesan. “Design and Implementation of Intelligent Controller Based Boost Converter for Electric Vehicle Applications” IEEE Student Conference on Research and Development (SCOReD), 16-17 Dec. 2014, USA, pp.1-6.

12 Chan, C. C., Alain Bouscayrol, Keyu Chen, 2010, “Electric Hybrid and Fuel-cell Vehicles Architectures and Modeling," IEEE Transactions on Vehicular Technology, Vol. 59, No. 2, 2010, pp.589-598.

13 Young-Joo Lee, Alireza Khaligh, Ali Emadi, 2009, “Advanced Integrated Bidirectional AC/DC and DC/DC Converter for Plug-In Hybrid Electric Vehicles,” IEEE Transactions on Vehicular Technology, Vol.58, No.8, October 2009, pp. 3970-3980.

14 Kang Miao Tan, Vigna K. Ramachandaramurthy, Jia Ying Yong. “Bidirectional battery charger for electric vehicle.” IEEE Innovative Smart Grid Technologies – Asia (ISGT ASIA) 2014.

15 Liping Guo, John Y. Hung and R.M. Nelms, “Comparative Evaluation of Linear PID and Fuzzy Control for a Boost Converter,” Industrial *Electronics Society, 2005. IECON 2005. 31st Annual Conference of IEEE*, 6-10 Nov 2005.

16 Tarun Gupta, R. R. Boudreaux, R. M. Nelms, and John Y. Hung, “Implementation of a Fuzzy Controller for DC–DC Converters Using an Inexpensive 8-bit Microcontroller,” *IEEE Transactions on Industrial Electronics*, Vol 44, No. 5, October 1997.

17 Begam, Shaik Ruksana; Burthi, Loveswara Rao; Depuru, Shobha Rani, “Adaptive Neuro-Fuzzy Sliding Mode Controller (ANF-SMC) to control speed, electromagnetic torque (EMT), Stator Current, and Back EMF using PMBLDC motor (PMBLDCM) in Electric Propulsion of Electric Vehicles” Przeglad Elektrotechniczny. 2023, Vol. 2023 Issue 8, p49-62. 14p.

18 Chander, S.; Agarwal, P.; Gupta, I.; "Design, modelling and simulation of DC-DC converter for low voltage applications," *Sustainable Energy Technologies (ICSET), 2010 IEEE International Conference on*, vol., no., pp.1-6, 6-9 Dec. 2010.

19 Ruksana Begam Shaik and Ezhil Vignesh Kannappan, "Application of adaptive neuro-fuzzy inference rule-based controller in hybrid electric vehicles", Journal of Electrical Engineering & Technology, Sep 2020, Vol 15, No 9, pp 1937-1945.

20 S. M. S. H. Rafin, R. Islam and O. A. Mohammed, "Overview of Power Electronic Converters in Electric Vehicle Applications," *2023 Fourth International Symposium on 3D Power Electronics Integration and Manufacturing (3D-PEIM)*, Miami, FL, USA, 2023, pp. 1-7, doi: 10.1109/3D- PEIM55914.2023.10052532.

21 M. R. Haque, K. M. A. Salam and M. A. Razzak, "A High Gain Cascaded DC-DC Boost Converter for Electric Vehicle Motor Controller and Other Renewable Energy Applications," *2022 IEEE International IOT, Electronics and Mechatronics Conference (IEMTRONICS)*, Toronto, ON, Canada, 2022, pp. 1-5, DOI: 10.1109/IEMTRONICS55184.2022.9795806.

22 K. P. Suresh, R. S. Kumar, C. Kathirvel, N. K. Balaji, V. S. Ajith Kumar and N. Agathiyanathan, "Switched Capacitor Based Voltage Boost Converter for Electric Vehicle Applications," *2021 7th International Conference on Advanced Computing and Communication Systems (ICACCS)*, Coimbatore, India, 2021, pp. 1205-1208, DOI: 10.1109/ICACCS51430.2021.9441761.

23 S. A *et al*., "Distinguished DC-DC Converter for an Electric Vehicle," *2022 6th International Conference on Computing Methodologies and Communication (ICCMC)*, Erode, India, 2022, pp. 578-582, DOI: 10.1109/ICCMC53470.2022.9753880.

24 Y. Guttula and S. Samanta, "Modeling and Control Implementation of Interleaved Coupled and Uncoupled Boost Converter for EV Drive Applications," *2021 IEEE 18th India Council International Conference (INDICON)*, Guwahati, India, 2021, pp. 1-6, DOI: 10.1109/INDICON52576.2021.9691491.

25 P. S. R. Nayak, K. Kamalapathi, N. Laxman and V. K. Tyagi, "Design and Simulation Of BUCK-BOOST Type Dual Input DC-DC Converter for Battery Charging Application in Electric Vehicle," *2021 International Conference on Sustainable Energy and Future Electric Transportation (SEFET)*, Hyderabad, India, 2021, pp. 1-6, DOI: 10.1109/SeFet48154.2021.9375658.